Chapter 2

Theoretical Background

2.1 RAIN

Rain is the liquid form of atmospheric water vapor content. Rain can form in several different ways. The formation of rain is dependent on the type of cloud, i.e. cold or warm. Raindrops are created in case of warm clouds in two main processes. One process is condensation and the second process is collision and coalescence. Condensation starts with the creation of small raindrops whose size is up 10μm radii approximately. Collision and coalescence are with larger rain drops.

2.2 FORMATION OF WARM CLOUDS

2.2.1 Condensation

The method of condensation begins with the gradient of warm air parcels. This result in air increasing and adiabatically cooling continuously, ultimately it reaches saturation. Because of continuous growth of parcel it will become supersaturated. A cloud of tiny water droplets forms as water vapor condenses onto some of the aerosol in the air. The droplets could also form due to impulsive nucleation where the aid of aerosol is not required. Impulsive nucleation is described as a process of chance collisions of water droplets in vapor phase coming together to form small embryonic water droplets [20].

2.2.2 Collision and Coalescence Condensation

Forms small droplets, where as the collision and coalescence process creates larger droplets [20]. The fall velocity of larger droplets is greater than smaller drops. Faster droplets are likely to collide with slower droplets in their path. However, not all droplets necessarily collide, since many of the smaller drops may follow the stream lines around the larger ones. It is not guaranteed that colliding droplets will coalesce with one another as the droplets may bounce off a layer of air trapped between the two. Alternatively the resulting drop could become unstable and breakup. If the cushion of air is squeezed out from between the drops before rebound can occur, the two surfaces make physical contact and coalescence will occur.

2.3 FORMATION OF COLD CLOUDS

A cloud that exists above the zero-degree isotherm level is typically called a ‘cold cloud’. It may contain both ice crystals and super cooled water droplets. Super

cooled droplets are water droplets that exist in clouds even though the temperature may be below 0^{O}C.A mixed cloud contains both ice crystals and super cooled water droplets, a glaciated cloud contains only ice crystals. Rain can form in cold clouds by vapour, riming or aggregation. Growth by vapour can not produce significantly large ice crystals. Ice crystal growth can occur by riming, where super cooled droplets that collide with ice crystals increasing the mass of the ice crystal. An ice crystal can also grow by aggregation where ice crystals collide and adhere to one another. Growth by riming and aggregation can produce a wide range of particle sizes, which melt to create larger rain drops.

2.4 RAIN CELLS

In the present work a rain cell is defined as the region of space composed of connected points where the rainfall rate exceeds a chosen threshold. There have been many studies in to the size and shape of rain cells using radars [21][22][23]. There have also been studies using long-term time series measurements made from rain gauges (with a time resolution such as 1 minute), which are used to estimate rain cell sizes using the synthetic storm technique [24].

The shape of a rain cell is generally irregular at the ground; however investigators have compared the perimeter of a rain cell to an ellipse. The statistics of rain cell geometry were independent of their location and threshold with an average ellipticity factor of 0.5[25]. The ellipticity infers that, on average, rain cells were twice as long as they were wide.

A model could be used to represent a measured rain cell. There are several models that have been derived to estimate rain cells. Some profile models are based on cylindrical or Gaussian shape [26][27]. Two well-known rain cell models include the EXCELL model [28] and the HYCELL model [29]. The EXCELL model describes the variation in rainfall rate within a cell as exponential, with circular or elliptical profile. The HYCELL model is a hybrid cell that combines exponential and Gaussian shapes. The Gaussian component models the high-intensity, convective rainfall rate and the exponential component represents the surrounding widespread rainfall. Both these models may be defined only by a few parameters, which have

significant advantages including reduced storage space and computational time when processing the cells in comparison to complete rainfall data.

Rain cells could be used to improve the effectiveness of propagation models, especially for systems with multiple paths, when predicting attenuation due to rain. The signal fade prediction process can greatly improve the effectiveness of fade mitigation techniques [30].

2.5 PHYSICAL CAUSE OF RAIN ATTENUATION

Propagation impairments of radio waves signals above 10 GHz is mainly because of the contribution of different troposphere elements which lies about 10Km to 20Km above the earth surface which extends to lower heights in temperate regions and more in tropic environment. Radio waves signals below 10GHz are mainly effected by the Ionosphere and degradation of wave due to constituents of Ionosphere (50-100Km). Ionosphere is extreme transparent for the frequencies above 10GHz.the factors which effect the earth space path for Ku and other higher frequencies are:

1. Impairment due to Rain

2. Impairment due to Gases

3. Impairment due to Clouds

4. Impairment due to Troposphere Scintillations

2.5.1 Impairment Due to Rain

Link availability of the earth space path mainly limited by the rain attenuation .Atmospheric Rain fall majorly categorized in to two types such as ***straight form rain*** and ***convective rain*** .Strightform rain is formed due to the cloud layer with wide spread rain and snow fall. Convective rain is due to vertical air currents with high rain intensity , thunders and lightning. Convective rain is more important for the satellite communication because of which the link outage period depends, mostly in the tropical environment in countries like India rain fall is only convective type .Strightform rain covers wide area with uniform and low rain intensity while convective rain is for less coverage with high rain intensity. Straight form rain generated by the snow because its intensity is low and is always less than 10mm/h this creates a constant rain attenuation of the slant rain path over the entire path. Convective rainstorms are complex, and have both vertical and horizontal

structure .The falling drops collides with the other drops and causes the size of the drop to increases which leads cross polarization.

2.5.2 Stratiform and convective rain

Rain fall can be categorized in to two types, first one is stratiform and second one is convective. Convective rain precipates from cumulus and cumulonimbus clouds while stratiform rain fall from Nimbostratus clouds [31].

2.5.2.1 Stratiform Rainfall

Stratiform rain is caused by frontal weather systems converging into areas of low pressure, in the situation when warm air meets cool air. A warm front arises from warm air overriding cool air, as the warm air raises it cools leading to precipitation. Cold fronts dislodge masses of warm air, which leads to more intense but shorter rainfall. Generally, Stratiform is more widespread rainfall that usually occurs for rainfall rates below $5mmhr^{-1}$. Stratiform rain occurs in clouds with extensive horizontal development, such as nimbostratus clouds, rather than vertical development.

2.5.2.2 Convective Rainfall

Convection occurs when a moisture content of atmosphere is heated above the temperature of its surroundings causes significant upward movement, which eventually leads to the formation of convective clouds. Convective rainfall also occur from cold fronts. A cold front undercutting warm air dislodges masses of air at a rate higher than the steady rise of air at a warm front. The air generally more unstable and leads to the formation of cumulonimbus clouds. Orographic uplift, when air is pushed from a low elevation to a high elevation over rising terrain such as mountains, can lead to considerable upward movement and convective rain. Convective rainfall usually consists of more number of, heavier raindrops, which usually occurs at rainfall rates above $10mmhr^{-1}$ over a short time period, and when the atmosphere is more unstable.

2.6 LITERATURE SURVEY

Major study in this work is concentrated on how rain affects on communication link, group of Impairment levels are grown up when the frequency of operation increases. Degradation of radio wave in rain media depends on the size and shape of the rain drop that is provided by the drop size distribution. The above

parameters are estimated based on polarimetric radar measurements, Gamma distribution was used to extract the size, shape, and DSD based on forward and backward scattering by drops using Radar Reflectivity and Differential radar reflectivity parameters [1]

Optical disrometer is the instrument used for the measurement of particle size and velocity based on amount of obstacle for a laser ribbon beam and how much time it was continued. Impact technique is the earlier method for measuring size and velocity of the particle but it needs large efforts to complete the evaluation. Joss waldvogel disdrometer work on impact technique with improved method. Another method is based on imaging using video line-scan cameras. Third method based on variety of scattering and single particle counters it includes extinction probes, forward scattering probe and also phase –Doppler instrument.[2].Accuracy of Z-R relation was improved by using RMSE[51].

Conversion of radar reflectivity as rain rate is the major part of the attenuation studies that explains about the empirical relation between the radar reflectivity and rain fall and also the some of power law relation between Z&R. Worldwide 69 power law relations are proposed depending on environmental conditions, out of which it is possible to use four for 'orographic' rain fall, five for 'thunder storm' rain fall, ten for 'widespread' or 'stratiform' and six for showers [3]. The remaining 44 empirical relations are unambiguously not associated with any type of rain fall for this study Marshall Palmer exponential relation and Battens relation was used for the conversion of radar reflectivity to rain rate. Drop size distribution $Nv(D)$ can be estimated by using exponential Distribution, Gamma distribution and lognormal distribution. The Parameters of Drop size distribution are No($mm^{-1}m^{-3}$) is $Nv(0)$ and slope factor ∧(mm^{-1}) ,sometimes it is possible to calculate the Drop size distribution from the rain fall velocity v(D) in terms of sample of rain *drop arivalprocess* [3]. C. R. Williams and K. S. Gage[48]in the 2009 work on convolution and deconvolution methods which are the two inverse methods used for DSD estimation. These methods work with one movement cost function and point-by-point cost function.DSD parameters are retrieved by using 42 different models for each set of radar data [48].

Two antenna systems techniques was used for the measurement of co-polar and cross-polar component of the signal. The output of the both LNBF's are given to the spectrum analyzer and then to the pc through data logger. The rain rate is measured from optical rain gauge (ORG-815-DA) and the DSD measurements from a disdrometer (RD 80).The calibration of satellite signal of both co-polar and cross-polar component have been done using a Ku band signal generator and rotary vane attenuator. This experiment was done to measure the amplitudes of the co-polar and cross-polar components, rain rate & DSD and to study the phenomenon of rain attenuation, depolarization and scintillation[4].

From the measured parameters, we observed that in tropics, it was found that at low to medium rain rates, the prediction models works well with the measured rain attenuation but at high rain rates, they tend to deviate. The Ramachandran and Kumar model[5] works well in predicting the rain attenuation at high rain rates as well, in tropical region.The results obtained can be used to guide the design of slant-path communication systems in South East Asia countries.

The analysis of long-term and short-term scintillation clearly shows that it doesn't affect the degradation of Signal-to-Noise ratio. The slope of $f^{8/3}$ achieved is compared with Kolmogorov spectrum and is clearly shows that the scintillation that occurred was without any rain attenuation. The scintillation is moderate during rainy season and very low during the dry season. So the fluctuation caused by tropospheric scintillation doesn't seriously affect (seriously) the radio wave transmission. The raw data is converted to signal level from quantization levels using fifth-order calibration polynomial. Then scintillation amplitude is extracted by passing the above signal through a Butterworth digital high-pass filter of sixth order with cut-off frequency of 0.06Hz [6].

Some researchers work on antenna effects on received Ku band received signal during rainy period with different elevationangles.During the experiment, the average attenuation is 2.81dB at very heavy rain rate. The results state that the attenuation caused mainly due to the wetness of the feed than the wetness of the reflector. The attenuation due to wetness of the reflector depends on the diameter and roughness of the reflector and the thickness of the water layer on the reflector. The attenuation caused by the water layer on the reflector was 0.2 dB at 12.4 GHz [7].

Equatorial Rainfall Measurement For the location USM (5.17^{o} N, 100.4^{o}E) according to the obtained results, the available ITU-R (2005), CRANE rain rate and rain attenuation models are often not suitable for equatorial climates. There is a high correlation between the rain rate and attenuation exceeded values in average years that would be useful in finding the fade margin [8].

Ku band attenuation prediction for the location Hassan, India (13.07^{o} N, 76.08^{o} E) measured Rain attenuation is compared with ITU-R, Excell, Karasawa, Leitao-Watson and DAH models. The ITU-R model underestimating the rain attenuation for Hassan location and the other models result in either underestimating or overestimating. For the attenuation measurement Rain attenuation is obtained by subtracting a reference level from the measured received signal level. The reference level is obtained by averaging the entire received signal level data on each month and at each place during no rain term. Predicted rain attenuation is calculated using the input requirements frequency, latitude, longitude, polarization, elevation angle, station height, antenna diameter, and other meteorological parameters along with the ITU-R data base files. Most of the input values used in the simulation are taken from the ECMWF data [9][49] .

When comparing the prediction models with the measured values, the prediction models do not work well in tropics, because they were developed in temperate climate regions, The ITU-R P.618 for rain attenuation prediction appears to work well down to outage times up to 0.01% of an average year. In order to get more accuracy, more attenuation measurements are required for tropical climates [10].

For the location Bangkok (13.7^{o} N, 100.7^{o} E) Cumulative distribution of rain attenuation and rain rate are obtained and are compared with the prediction models. The ITU-R model agrees with the measured attenuation at medium to low rain rates but tend to deviate at higher rain rates. This is because, lack of measurement data to model the rain attenuation for different climate regions [11].

Signal fluctuations occurred due to scintillation and rain attenuation are studied by using Wavelet analysis for the region Kolkata (22.34^{o} N, 88.29^{o} E) The time evolution of the wavelet power for fast and slow fluctuations corresponding to the two phenomena has been depicted in the wavelet spectrum. The power is much higher for large scale wavelets compared to small scale ones, showing that the

attenuation is much more dominant phenomenon compared to the scintillation. The results from high pass filtering is in power-law relation with the attenuation during few rain events. The relationship, as obtained in those cases, indicates that both the thin and thick layer turbulence can occur in the raining conditions at the present location [12].

Phenomenon of depolarization of a Ku-band satellite signal caused by rain has been studied in which the attenuation of the copolar component and the enhancement of the cross-polar component signal have been measured at one of the tropical location. Presents a technique of sensing the rain-induced depolarization effect of a low fade margin satellite signal [13]. Shun-Peng Shih and Yen-Hsyang Chu work on Ka band beacon signal from ROCSAT-1 in the year 1999, is the LEO satellite.LEO satellite changes its position with respect to the earth station antenna leads to the variation of propagation effects and link reliability also varies. Total attenuation was calculated by estimating the rain rate with different percentage exceedance values[52].

Rain rate and Rain attenuation for Ku-band (14/12GHz) is measured and analyzed. These measurements are compared with ITU-R prediction models. The difference between predicted and measured values are analyzed to present a modified algorithm and to correct the ITU-R forecasting model. This experiment suggests that we need to have long term data in order to develop good relation between rain rate and rain attenuation at different stations[14][47].

The microwave propagation in atmosphere is simulated by means of the MPM 93 model using a software simulator for the performance evaluation of NDSA (Normalised Differential Spectral Absorption) with two counter rotating satellites. This software tool process atmospheric vertical profiles (Pressure, Temperature, Water and Liquid contents).The chosen location was the University of Florence at frequency of 17.2 5 and20.20GHz for the LEO satellite [15].

Rain attenuation also varies with drop size. Drop Size Distribution (DSD) is measured along with rain attenuation and rain rate for three years. By studying of these measurements it is observed that the density of drops with larger diameter dominates in pre-monsoon season. The analysis of three years reveal that the pre-monsoon months experience a greater attenuation than the monsoon months for the same rain rate because variations in DSD. These measurements are made with Joss-

type disdrometer (RD80), optical rain gauge (model: OSI ORG-815-DA) by using Marshall-Palmer and Laws-Parsons models and also Ku-band beacon was measured [16][54].

Prediction of scintillation with low elevation angles at frequencies 11/14 GHz for standard atmosphere, depends only on meteorological conditions irrespective of method used. For the higher elevation angles ($\theta >= 5^{o}$), the amount of scintillation is dependent on humidity, temperature, frequency and antenna diameter. Among all the elevation angle has greater impact on scintillation [17].

Short term scintillation effects were measured by using log logistic method, log normal and gamma methods. Under stationary conditions the amplitudes of short term period scintillation take the Gaussian distribution which describes the fading of the signal. Prediction of amplitude scintillation for Ku band was implemented by using Karasawa Model and Moulsley-Vilar Model using median and variance respectively. For long term estimations with high elevation angles lognormal distribution is the best suitable method [18].Scintillation varies with temperature and humidity level, in *Kuala* Lumpur, Malaysia. Scintillation peak to peak amplitude variations for morning, evening and midday for the period of eight months, peak to peak amplitude for the midday with 1.02dB.Scintilaltion peak to peak amplitude fluctuations are more in period from October2011 to December2011[50].

In the year 2010 Mani deep[19] discussed about the various scintillation prediction models like karasava model, ITU-R model, van de camp model and otung model. Van de camp model slightly deviates from the ITU-R in terms of scintillation standard deviation. Otung model slightly deviates from the ITU-R in terms of order of elevation angle dependency .

Because of the unavailability of the actual signal measurements, rain data values are recorded for the accurate prediction of rain attenuation in any region. The work done by the people in the Kolkata University based on the two years continuously recorded rain data using Simple Attenuation model (SAM) ,ITU-R model. The obtained results are compared with the measured data and predicted one, each model deviates from the measured value.

In the year 2011, L. S. Kumar, Y. H. Lee, J. X. Yeo, and J. T. Ong work on Z-R relation based on nine rain events for convective rain cases , striteform rain and

transition cases also using Gamache-Houze method, a simple threshold technique, and the Atlas-Ulbrich method. In Atlas-Ulbrich method the integration parameters like R, Z, Do and Nw are used along with Gamma model parameter μ.for Singapore region Z-R relation coefficients were estimated based on type of rain fall.The rain parameters are estimated from radar data, at any case the measured rain from radar data is always less than the rain data measured from Disdrometer[40].

For the regions where large convective rain are occurred it is necessary to study and investigate the rain effect on higher frequencies. But unfortunately the actual signal was not available directly because of that attenuation studies are based on meteorological parameters. With the usage of simple approach to generate the rain attenuation time series for experimental location particularly for the tropical environment the effective slant path length is independent on rain rate or intensity for all existing attenuation models. A. Adhikari, S. Das, A. Bhattacharya, and A. Maitra work on effective slant path length calculation using power law equation which varies with rain fall R [41].

Rain fall rate was recorded with integration of either 1 hour interval or on twenty four hours basis, existing attenuation models work with one minute integration .Estimation of attenuation using attenuation models is mandatory to convert any integration period to one minute integration period. J. S. Man deep, S. I. S. Hassan discussed about the conversion using different methods like segal method, Burgueno et al. method, Chebil and Rahman method, Joo et al. method, Moupfouma and Martin method. Selected experimental locations are KMITL, ITB, USM, UniTech, USP, ADMU and USM, out of all methods given segal method is the best suitable for the tropical regions.Chebil rahman(1999) method gives an error of less than 6%for the locations with a 0.01% probability of existence of rain. Moupfouma and martin (1995) method for 1% occurrence of rain under estimate from the measured value and closes to measured value at 0.01% and 0.1% occurrence. Joo et.al method developed in 2002 is not useful for the tropical region [42].

Rain attenuation studies were conducted in Kuala lumpur (3.30 N, 101.70 E) for the study of Rain fade at a frequency of 10.982 GHz with the elevation angle of 77.40 for the reception of MEASAT3(91.50E).As per the ITU-R Model Rain fade slope S was measured with the integration period of 1 sec, and probability distribution

function was studied with S=0.01with zero offset fit. Hassan Dao, Md. Rafiqul Islam and Khalid Al-Khateeb[43] proposed a new fade slope value S=0.0023 for the tropical environments for Ku band frequency.

Rafiqul MD Islam, Yusuf A Abdurrahman and Tharek A Rahman[44] work on to develop new method by modifying the coefficients with moving average technique and non linear multiple regression have been investigated to fit for different time percentage values for all the locations. The proposed new model was tested against the measured data for all the tropical location and the new method is the best suitable compared with IRU-R..

Polorometric radars are used for the rain attenuation studies through radar reflectivity parameter, which is power related to rain fall. Seliga and Bringi in 1976[46] method attracts many communication engineers, but it involves tedeious process to calculate rain rate R.F in the radar measurements the rain rate was measured by using empherical relation or retrieving the DSD parameters [45].

Animesh Maitra and Arpita Adhikari[53] work on co and cross polar signals for the Ku band in the year 2004 onwards by considering two different rain events. Experimental setup was placed at Kolkata (22°34′N, 88°29′E).Earth station pointing towards NSS6 satellite with elevation angle of 62.5^{o}. The observed copular attenuation is about 11dB and Cross polar attenuation is about 9dB. Depolarization of Ku band signal is the cause of Differential phase shift due to forward and backward scattering. Depolarization depends on Scattering and size of the raindrop.

Earlier specific attenuation calculation was made by approximating the rain drops with uniform size and raindrops of same size which are uniformly distributed in space. To sum the scattered fields in space single scattering theory was used, frequency below 2GHz Rayleigh scattering and for higher frequencies Mie scattering theory was used and also the the drop size distribution was same on the line of sight path for the same surface. Large falling drops are unstable but they approximated as spherical shapes to measured the scattering. Crane[57] revised all the experiments which were conducted between 1964-1970for the development of accurate experimental model for measuring specific attenuation, he noticed a deviation between the theoretical analysis and experimental results due to improper recording of the rain fall measurement. As per the crane model specific attenuation was

independent on polarization of the signal. Surface rain fall data can give only rain attenuation only.

In the year 1976 R. R. Rogers work on attenuation calculation using drop size distribution and Mie scattering theory by using total attenuation offered by the spherical cross section of the rain drops. In Drop size Distribution Drop break up play a critical role, drop size distribution increases with the size of the drop. Drops may breakup due to collision between the drops. If the drop radius is greater than the 1.5mm it not sure drop can reach as a single drop and if the size is greater than 3mm its radius is unstable tend to break up and produces small drops.DSD can also be estimated from radar reflectivity, it will linkup with the rain rate as given by the marshal palmer distribution [58].

Arun k verma et al have presented the measured RSD and observed that thunderstorm rain contains rain drops of larger sizes as compared to shower rain. The Laws and Parsons RDSD model proposed by Marshall and Palmer are suitable for temperate climate, which overestimates both small and large rain drops. The log-normal RDSD model based on the measured data at dehradun has been compared with log-normal RDSD models of Brazil and Nigeria. It is observed that the RDSD model agrees closely with existing models. The results presented indicate log-normal distribution seems to be appropriate for tropical climate like India [72].

K I Timoty[73] have developed a mathematical model for the calculation of rain rate using the rain drop size distribution. The proposed model is validated with the measured RSD over the Indian regions .

Tat-Soon Yeo et al have developed a new negative exponential rain drop size distribution model suitable for tropical climate and for 10GHz – 40GHz and emploting horizontal, vertical and circular polarization. This model was developed based on the data collected over 10 years [74].

K. Isaiah Timothy et al have corrected the dos software provided by Distromet and the presented modification can correct up to 10% [75].

Gamantyo et al have derived the coefficients of the desired power-law relationships using the DSD averages from two measurement sites. The coefficients obtained are found to differ slightly from those recommended by the ITU-R due to differences in the method of DSD measurement and parameter derivation [76].

Carlo Capsoni et al have presented an improved version of the EXCELL rain attenuation model. The new model allows the calculation of attenuation contributions from stratiform and convective rain separately. Two different physical rain heights are also derived from the ERA-15 database, are used for stratiform and convective rain [77].

Maitra has obtained rain attenuation and attenuation distribution using the measured rain drop size distribution and the ITU-R model doesn't fit well and we need more data to find out the DSD effect on the signal attenuation [78].

Robert. K. Crane[79] has documented existence of attenuation and depolarization effects and how to estimate attenuation from rain rate.

R. R. Rogers has reviewed that precipitation has become a serious source of attenuation at higher frequencies. The current status of rain cell models is reviewed and suggestions for future research are offered [80].

Robert K. Crane has presented a model for prediction of attenuation by rain and it performed well in predicting the attenuation [81].

TorleiV Maseng [82] have developed a dynamic mathematical model of rain attenuation and fluctuations

Yoshio Karasawa [83] have presented a simple conversion method of 1hr- rain rate data to 1 min- rain rate distribution. Prediction accuracy of the method is evaluated and good accuracy is confirmed and can be used where 1min- rain rate is not available.

Wei Zang[84] have obtained specific phase shift as well as the specific attenuation by the Mie theory applied to the melting snow particles and is useful for satellite earth communications and radar remote sensing.

K. I. Timothy[85]have presented the RSD during various rainfall types. a and b co-efficients for $A= aR^b$ are calculated for each type of observed RSD.

A. Paraboni [86]dealt with the severe propagation problems in designing the future satellite communication systems in Ka band and with some possible advanced solutions based on the knowledge of local climatology [86].

L. Raynaud[87], have studied the characterization and modeling of the melting layer in order to predict its effects on spatial communications. Some models exist, are not satisfactory. So a new calculation for scattering by a particle has been introduced.

David A. De wolf[88] has presented a new analytical function for the distribution density of rain drop diameters implied by the measured Laws-Parsons distribution of the volume fraction of water in rain. It yields results that differ from those obtained via the marshall-Palmer exponential function of drop diameter.

A. D. Panagopoulos[89]has presented a method to predict the differential rain attenuation statistics on converging links based on model convective rain cell structure of the rainfall medium. It has been tested with experimental results from ITU-R SG3 data bank and agrees well.

Margarita Baquero[90] have compared the data from NCDC and NWS rain gauges to that of the distrometer and derived the β co-efficients for Z-R algorithms. The derived co-efficient α in X-band for convective and stratiform rain is approximately double of that found in Australia during wet season even though the co-efficient β is similar to those of that study.

M. A. Awang [91]have compared the rain attenuation measurements at different locations with various DSD models. The use of DSD established for other countries result in prediction error when applied.

Yong-Ho Park[92] introduced a new model for DSD, based on the measurements performed in Chungnam National University. It was found that the log normal distribution is the most adequate for describing DSD than other models. The results of the calculated rain attenuation using proposed DSD model revealed an excellent agreement with the measurement data.

2.7 FALL VELOCITY AND SHAPE OF RAINDROPS

2.7.1 Velocity

The shape and terminal velocity of raindrops are very important factors for the calculation of rainfall rate and resulting radio wave attenuation. Gunn and Kinzer[32] determined a method to estimate the fall velocity of raindrops. The experiment involves a dropper capable of producing water drops of size varies from 0.1 to 100,000μg. For the measurement an insulated ring-shaped electrodes are used. When droplets detached from plunger, they would fall through it and a free charge would be placed on the droplet. To calculate the fall velocity, a drop was passed through the two inducing rings approximately one meter apart. A free electrical charge, deposited on each droplet, generated a pulse on each inductive ring as it descended. The time difference and spacing of the rings were used to measure the average velocity. The drop masses were determined using a highly-sensitive chemical balance.

Using these results [141]and similar work by other authors, for example, D Atlas and Sekhon [141] an expression for the terminal velocity was calculated and is shown in equation (2.1). The results followed the pattern that the larger the raindrop the faster it would fall. However, as the diameter of the drop increases above 2mm the increase in velocity begins to decrease. Once the diameter is close to 4mm, the drops terminal velocity reaches a maximum.

$$V(D) = 9.65 - 10.3 \exp(-0.6D) \qquad (2.1)$$

D is the drop diameter given in mm and V (D) is the raindrop velocity of drop diameter D in $ms^{-1.}$

2.7.2 Shape and Size of the Rain Drop

Raindrops vary in both shape and size [34]. A water drop with no noticeable motion relative to the surrounding air will assume a spherical shape due to the surface tension of water. The surface tension results in the inside spherical pressure of the

drop being greater than atmospheric. When the drop falls, unequal pressure forms over the surface. Pressure increases at the bottom of the drop, and decreases at the top and sides.

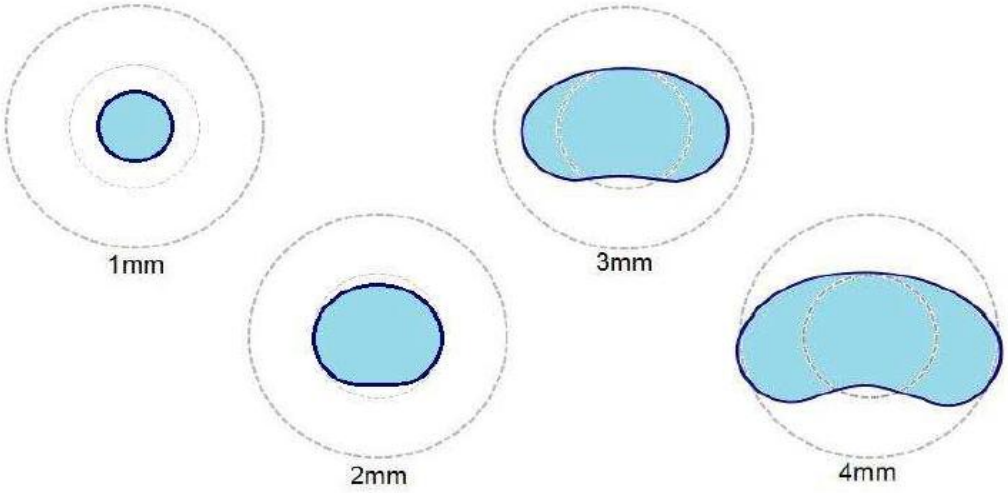

Figure 2.1. Rain drop shapes with size 1mm, 2mm, 3mm and 4mm

The pressure change deforms the water drop by flattening the bottom surface and spreading the shape sideways. The size of the raindrop effects the way in which the raindrop is deformed. Experimental results which investigate photographs of raindrops falling were obtained by Pruppacher and Beard [35]. Measurements showed that raindrops above 2.0mm in diameter were affected by the change in pressure on the outside of the drop and became oblate spheroidal in shape.

Figure 2.1 shows the different types of raindrop shapes for given sizes. Generally, raindrops larger than 8mm in diameter are hydro dynamically unstable and tend to break up, as observed by Pruppacher and Pitter [36].

2.8 BREAKUP OF RAINDROPS

Raindrops above 2mm in diameter become flattened on their underside in free fall and gradually change from a spherical to an almost parachute shape. If the diameter of the drop is greater than 5mm the parachute becomes a large inverted bag, with a toroidal ring of water around its rim. Studies have shown that the drop bag bursts to produce a fine spray of droplets; the toroidal ring breaks up into a number of

large drops, which forms an exponential raindrop size distribution[38]. A representation of this process is shown in Figure 2.2. There is some controversy over whether collisions between drops are the largest cause of breakup. It has been suggested that the number of collisions is not large enough for a stable distribution to emerge, and coalescence is thought to be the main ingredient[20]. The bursting time is also much smaller than the falling time.

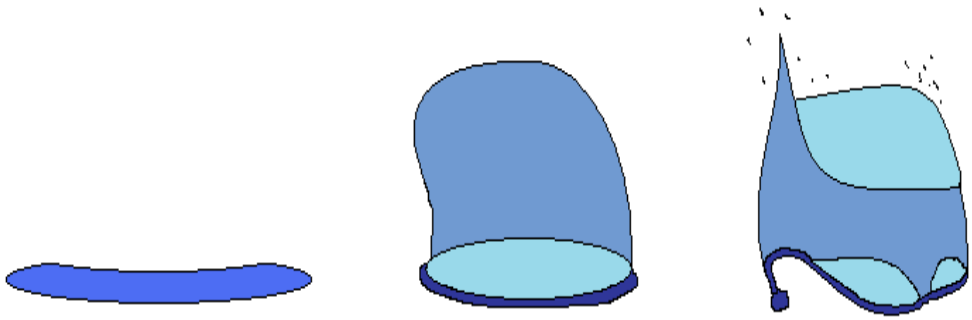

(a) (b) (c)

Figure 2.2. Rain drop shapes with their size (a) a Rain drop with >5mm diameter forming a parachute, (b) inverted bag shape rain drop,(c)Break up of rain drop.

2.9 RAINDROP CANTING ANGLE

Raindrops can fall with different canting angles, which will change the resultant fading levels for linear polarization on non-spherical raindrops and reduce polarization discrimination. Horizontal wind speed varies with height; therefore relative airflow to a drop is not even along the length of the drop as it is accelerated or retarded in the horizontal direction, canting the drop. Vertical wind gradients also result in a horizontal force on raindrops [37]. If the wind speed is constant and independent of height, the drops will assume the same horizontal speed as the surrounding air, therefore the relative airflow to the drop will be vertical. The canting angle is a function of the differential of the vertical wind profile, not the absolute value of the wind speed.

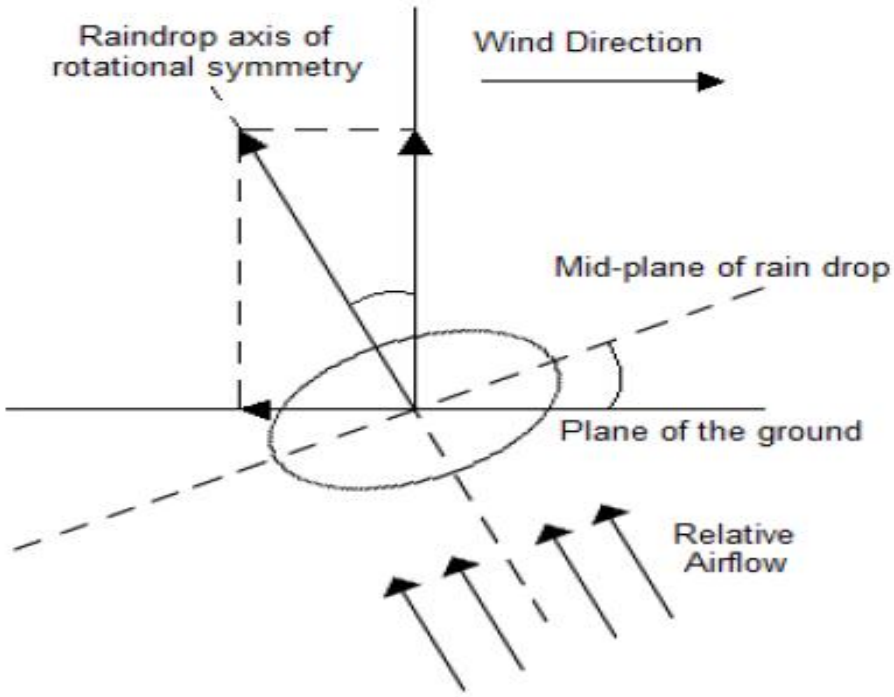

Figure 2.3. illustration of rain drop canting angle with inclusion of wind force

2.10 RADAR REFLECTIVITY

From the last 60 years weather radars are utilized as a tool to improve rainfall measurement in hydrology [3]. In recent time's study related to radars in hydrological measurements shows that the radar has a potential value to prepare better rainfall measurements. In almost all the locations for the measurement of rain fall rain gauge stations are available. Large data base is required for forecasting the rain attenuation. Joss and Waldyogel [59] discusses about the advantage of using radar for precipitation measument, it covers the large area. Z-R relation mainly varies with rain pattern that is either convective or stratiform sometimes combination of both. Event type is one of the major influences of Z-R relationship that must be studied accordingly. In addition, the experimental location also plays an important role in applying Z-R relationships to radar rainfall measurements. Various Z-R relationships are devloped according to the event types (convective, stratiform) and locations. Different equations are suitable for different atmospheric conditions. Thus, it is necessary to ensure the radar conversion system uses the correct/suitable Z-R equations for radar-rainfall measurement purposes.

"The measure of microwave energy returned to the radar after reflecting off particles in the atmosphere" expressed in Decibels, dBZ. Atmospheric particles those are rain drops or other metrological parameters. Radar reflectivity range varies between 0dBZ to 80 dBZ, Reflectivity scale always negative because of logarithmic scale. If the radar reflectivity is 0dBZ, very little or almost no energy is returned back, if it is 80dBZ maximum energy return. Return power from any object including metrological objects depends on cross sectional area of the object called "***radar cross section of the target*** " and is defined as the fractional area of the target which intercepting with the power which produces an echo at the radar [3].

Radar received power equation describes the amount of received power, radar characteristics, type of the target and ranging between the radar and target in this analysis. Rain drop will act as a target to the radar.Rain drop appear as an obstacle to an electromagnetic wave and the wave reflects from the obstacle which was measured by using OTT Parsivel Disdrometer as Radar reflectivity. Radar reflectivity is converted in to the rain rate using existing empirical relations.

Radar reflectivity Z is related to the size of drop and drop size distribution as

$$Z=\int_0^\infty D^6 N_v(D)dD \qquad (2.2)$$

Where Z [3] is the Radar reflectivity in dB ,D Drop size in mm and $N_v(D)dD$ represent the mean number of rain drops with equivalent spherical diameters between D and D+dD (mm) present per unit volume of air. V Represents the volume.

Rain rate R is related to the drop size and drop size distribution as

$$R=6\pi\times10^{-4}\int_0^\infty D^3V(D)N_v(D)dD \qquad (2.3)$$

Where v (D) represents the terminal fall velocity in still air(m/s).R is the Rain rate(mm/h).

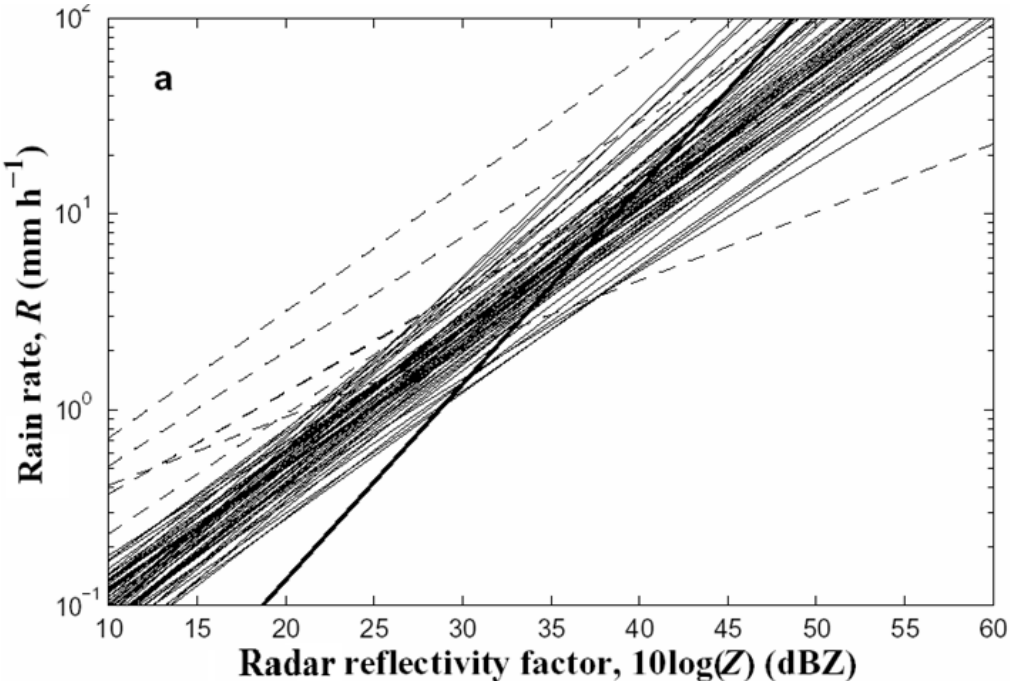

Figure 2.4. 69Power law Z-R relationships[3]including five deviating relationships as indicated by dashed lines, four of which have prefator a significantly smaller than 100 and one of which has an exponent b as high as 2.87.the bold line in the figure represents the linear relationship as proposed by the list[33][3].

Comparing the equations (2.2) and (2.3), it is interesting to note that Z and R are coupled by drop size distribution, consequently the power law relation of Z and R becomes fascinating for drop size distribution calculations [33][3] .

2.10.1 Empirical Rain Rate and Radar Reflectivity Relationships

In order to measure the Rain drop size distribution, there exists a empirical evidence that follow power laws of the form

$$Z= aR^b \qquad (2.4)$$

Where a & b are empherical coefficients that may vary from one season to other, one location to other location and also different for different rain types. Equation(2.4) gives the power law relation between Z&R, by taking arithmetic and geometric mean of the coefficients, a and b respectively.

$$Z=238R^{1.50} \qquad (2.5)$$

Equation (2.5) was proposed by battens in 1973 and Marshall Palmer proposed another power law relation between Z & R that is most suitable for most of the rain fall types and for most of the areas in the world.

$$Z=200R^{1.6} \qquad (2.6)$$

Marshall Palmer is the best suitable method for the tropical regions like India. In this work mainly it is discussed about the Radar reflectivity variation and estimation of rain rate from Radar reflectivity using the empirical relations and also the drop size distribution along with size and velocity estimation [33].World wide,69 power law relations are proposed depending on environmental conditions, out of which it is possible to use four for 'orographic' rain fall, five for 'thunder storm' rain fall, ten for 'widespread' or 'stratiform' and six for showers. The remaining 44 empirical relations are unambiguously not associated with any type of rain fall.

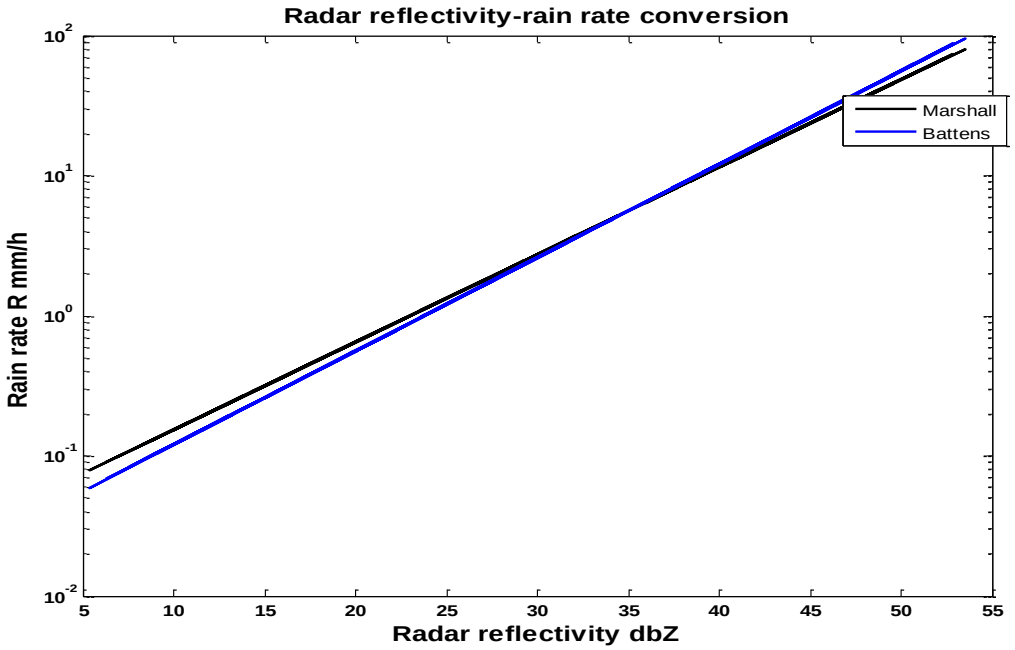

Figure 2.5. The bold line represents the Marshall et al and dashed line represents the mean Battens relation for the experimental data recorded at KLUniversity.

In this work Marshall and palmer relation is used which is suitable for rain type in our region[33]. To carry out the work, OTT Percival Optical Disdrometer was placed at KLUniversity, Guntur, and Andhra Pradesh, India. With the help of ASDO soft

ware package and an interfacing device(MOXA TC100) between RS232 and RS 485(2wire terminal in active) rain data was logged on the computer.

2.10.2 Rain Rate Calculation From Radar Reflectivity

Rain rate is calculated by neglecting wind effects, interaction between drops and by using empirical power law relation between Rain Rate(R) and Reflectivity factor (Z).Radar Reflectivity is taken from the data recorded in the OTT Percival Disdrometer. With the help of equation (2.4) the Rain Rate(R) can be measured. Under clear air condition radar reflectivity is negative rain intensity is zero and no variation in received spectrum amplitude. Attenuation due to rain for any EMwave depends on rain intensity and also on frequency of EMwave.

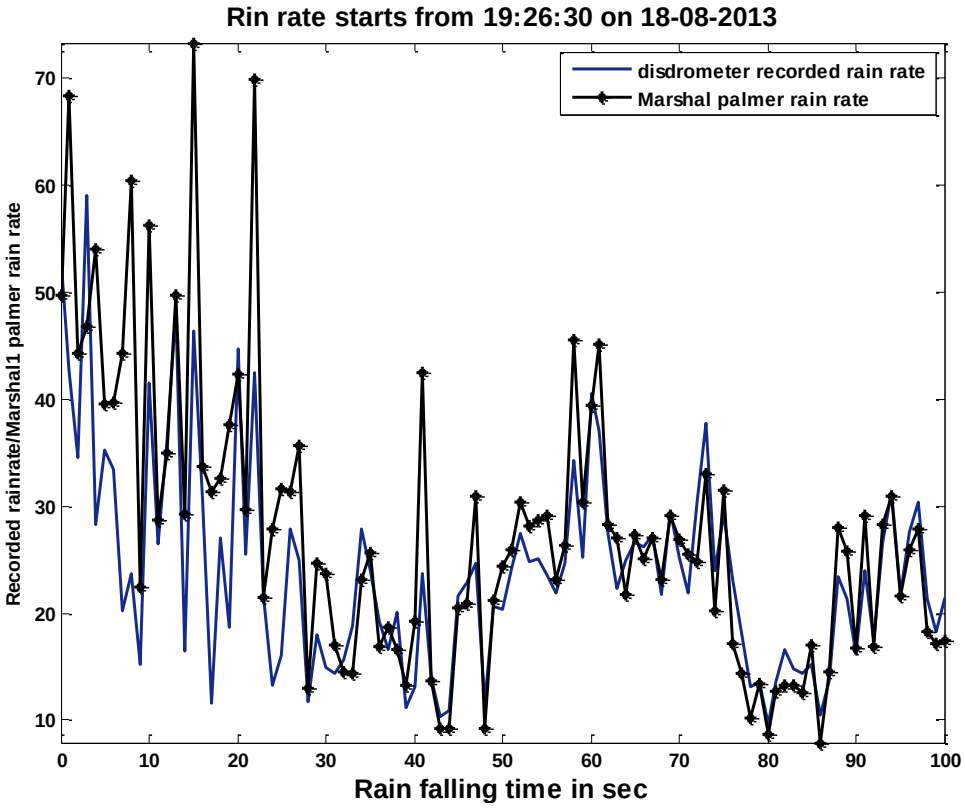

Figure 2.6 Solid line represents the measured rain rate on 18-09-2013 starts at 19:26:30; dashed line represents the rain rate calculated from measured Radar reflectivity using Marshall et al, power law relation

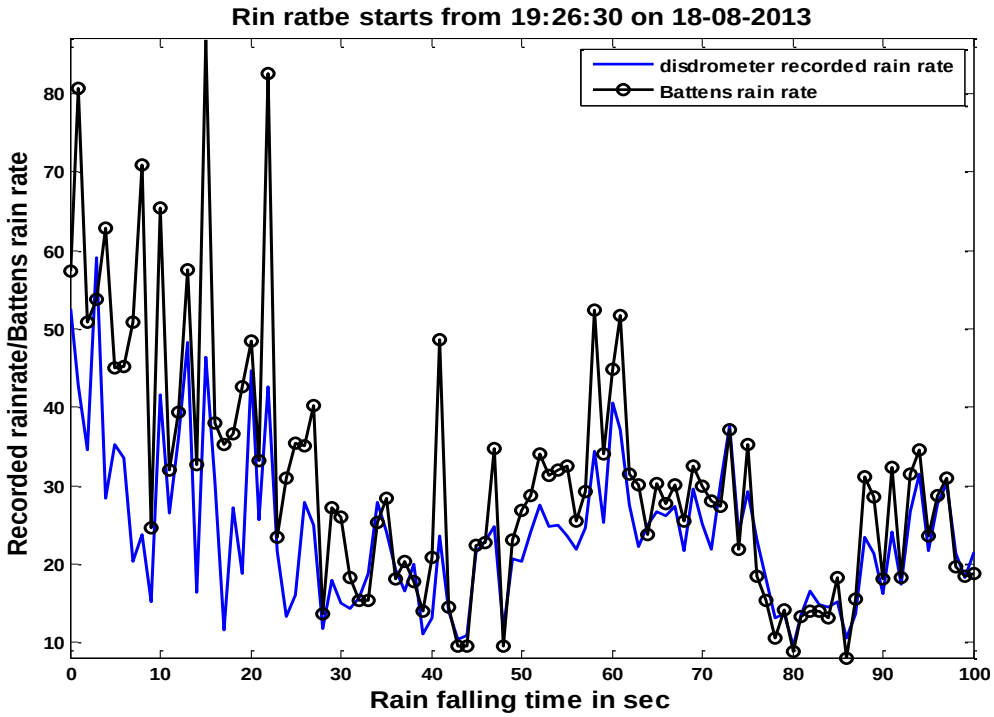

Figure 2.7 Solid line represents the measured rain rate on 18-09-2013 starts at 19:26:30, dashed line represents the rain rate calculated from measured Radar reflectivity using battens, power law relation

The Rain rate is calculated from radar reflectivity using Marshall Palmer relation and Battens relation. Marshall Palmer result is very close to the measured rain rate than Rain rate obtained from Battens relation, particularly at the point of sudden variations in rain intensity.

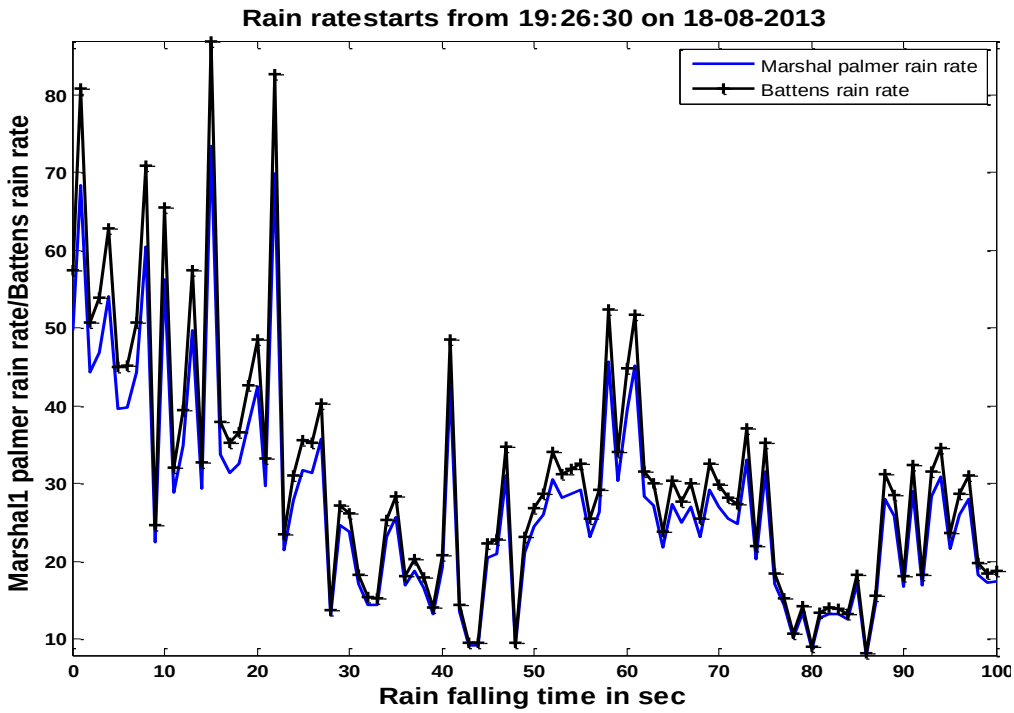

Figure 2.8 solid line represents the simulated rain rate using Marshall et al on 18-09-2013 starts at 19:26:30; dashed line represents the simulated rain rate from measured Radar reflectivity using Battens, power law relation.

Rain rate calculated using Marshall and palmer, Battens are shown in fig.2.6, where both gives the same rain rate for constant increment and constant decrement and are slightly differed by small value at sudden transition points.

2.11 PROPAGATION CHANNEL MODELING

The effectiveness of fade mitigation techniques can be improved with the use of propagation channel modeling. There are a variety of techniques used to model channel propagation in order to determine the total attenuation on a link. ITU-R P.618 -8: Propagation data and prediction methods required for the design of Earth-space telecommunication systems, N-state Markov chain models, Synthetic storm technique and two sample model and the propagation forecast engine are a few examples among many. Propagation modeling can be used to evaluate the behavior and quality of service of communication systems, and helps the implementation of fade Mitigation techniques [39].

2.11.1 ITU-R P.618-8

ITU-R recommendation P.618-8 estimates statistics of various propagation effects that should be considered in the design of earth-space links. Propagation effects such as absorption, scattering and depolarization by hydrometeors, absorption due to atmospheric gases, multipath effects and ionospheric effects (typically only notable below1GHz) can cause signal fade and need to be considered when implementing a satellite system to maintain a quality of service. Statistics for propagation effects provide an attenuation cumulative distribution function (CDF), which can be combined with further ITU-R recommendations to create an overall average annual attenuation CDF. Other ITU-R recommendations include rainfall rate, P.837-5, rain attenuation, P.838-3, cloud attenuation, P.840, and gas attenuation, P.676.

2.11.2 N-State Markov Chain Models

The N-state Markov model, Castanet et al. [2003], is based on two main components: a macroscopic model that has two states, rain or no rain: and the microscopic level, which fills rain events with attenuation time series. The macroscopic model is used to identify each rain event, based on two components, the probability of rain (typically based on ITU-R statistics) and the probability of change from rain to clear sky (typically defined by Paraboni and Riva [1994]). The microscopic model follows an N-state Markov model, where N states are used to define attenuation levels. A fade slope model is used to define the probability of a particular fade slope given an attenuation level.

This approach uses ITU-R models (such as ITU-R P837 - Characteristics of precipitation for prorogation modeling) to provide annual statistics of rain occurrences, therefore, shorter periods could demonstrate considerable variation. The microscopic and macroscopic models are independent, which does not allow the microscopic model information about the length of an event.

2.11.3 Synthetic Storm Technique

The synthetic storm technique, developed by Matricciani in 1996[137], takes a single site rainfall rate time series, typically from a rain gauge or disdrometer, and converts the values into an attenuation time series, based on a simple model of the vertical structure of precipitation. The model consists of two layers A and B. Layer A

is a uniform rainfall rate, as measured at the ground, and layer B represents the melting layer, where ice hydrometeors begin at the top and transform into raindrops at the top of layer A, to calculate an attenuation time series. The synthetic storm technique is based on work by Drufuca in 1974[138] proposing a similar method applied to terrestrial links in 1974, which was re-engineered for Earth space links.

2.11.4 Two Sample Model

The two sample model, developed by van de Kamp in 2002[139], can be used to generate attenuation time series for simulation or provide very short term (10 seconds) propagation channel forecasts. The model predicts the probability distribution of attenuation given the previous two samples and the relative change in time. The technique is an extension of the hypothesis of near-future attenuation level as a function of the previous samples, Dossi in 1990[140].